Available online at www.sciencedirect.com
ScienceDirect
Progress in Nuclear Energy 49 (2007) 385–396
PROGRESS IN NUCLEAR ENERGY
An International Review Journal
www.elsevier.com/locate/pnucene

Response functions for calculating axial power-density profiles in fuel rods using in-core neutron detectors

A.S.M. Sabbir Ahmed [a,*], J.K. Shultis [b], D.S. McGregor [c]

[a] German Cancer Research Center (DKFZ), Im Neuenheimer Feld 280, Department of Medical Physics in Radiology ECT-E0204, Room N117, Heidelberg D-69120, Germany
[b] Department of Mechanical and Nuclear Engineering, Ward Hall, Room 137-B, Kansas State University, Manhattan, KS 66506-2503, USA
[c] Department of Mechanical and Nuclear Engineering, Rathbone Hall, Kansas State University, Manhattan, KS 66506-2503, USA

Abstract

Micro-pocket fission detectors (MPFDs) have recently been fabricated and successfully tested as in-core flux monitoring devices in the nuclear reactor in Kansas State University. These detectors are sufficiently small to be inserted between fuel elements. Data from an MPFD array can be converted into a 3D power-density map of the reactor core for real-time flux monitoring. In the present study, the necessary mathematical models are developed that relate the power-density profiles in fuel rods to the MPFDs' response. The applicability of an inversion algorithm proposed for obtaining power-density profiles is also verified in this study.

PACS: 0168-9002

Keywords: Detector response function; Neutron detectors; Reactor power density; Inverse problems

1. Introduction

The response (e.g., count rate) of an in-core neutron detector depends on the average flux in the detector. The flux in a detector depends largely on the production rate of fission neutrons in adjacent fuel rods. The fission-neutron production rate at a location in a fuel rod is, in turn, proportional to the power density at that point.[1] From the responses of neutron detectors distributed throughout a reactor core it is possible, in principle, to determine the power-density profile $u^k(z)$ (W cm^{-3}) at an axial elevation z in fuel rod k. Using very idealized response function models, Shultis (2005) demonstrated that it was possible to determine the axial power-density profiles in fuel rods from count rate data produced by an array of in-core detectors.

Recently, micro-pocket fission detectors (MPFDs) have been fabricated and successfully tested as in-core flux monitoring devices in Kansas State University's TRIGA reactor (McGregor et al., 2005). These extremely small fission chambers (volume $\simeq 1$ mm^3) are extremely insensitive to background gamma rays and can operate in pulse mode

* Corresponding author.
E-mail addresses: a.ahmed@dkfz.de (A.S.M.S. Ahmed), jks@ksu.edu (J.K. Shultis), mcgregor@ksu.edu (D.S. McGregor).

[1] The contribution to the power released by the radioactive decay of fission products previously created in a fuel rod is of minor importance and is ignored in the present analysis.

0149-1970/$ - see front matter © 2007 Elsevier Ltd. All rights reserved.
doi:10.1016/j.pnucene.2007.04.001

over the full power range of the reactor. These MPFDs can be fabricated to respond primarily to thermal neutrons by using a fissile converter material or to only fast neutrons by using a threshold fissionable converter material.

From the responses of an array of in-core MPFDs, it is planned to infer the power-density profiles in the fuel rods for real-time monitoring of the power-density distribution in the TRIGA core. However, to infer power-density profiles for KSU TRIGA fuel rods, it is first necessary to obtain accurate MPFD response functions that relate the detectors' count rate (or responses) to the power-density profiles in the fuel rods. The MPFD response functions contain all the physics of fission-neutron transport and thermalization, the core geometry and composition, and the response characteristics of the MPFDs. The calculation of MPFD response functions for the TRIGA reactor is the focus of this study.

2. Modeling the MPFD response

In this section a specific model for the MPFD response function is developed for a reactor core containing K parallel vertical fuel rods, each with the same length $z_{\max}$ of fuel, located in a light water moderator ($z = 0$ is the bottom of the fuel meat). An array of N_{d} MPFDs are placed in the moderator throughout the core. The detectors are modeled as point isotopic detectors whose converter fissionable material is either fully enriched ^{235}U for thermal neutron detection or ^{232}Th for fast neutron detection. Also, for simplicity, it is assumed that the power density in a fuel rod has no radial dependence and varies only axially.

2.1. Detector response function

At elevation z in fuel rod k the power density $u^k(z)$ is proportional to the fission-neutron (fn) production rate density $S^k_{\mathrm{fn}}(z)$, namely, $S^k_{\mathrm{fn}}(z) = \kappa u^k(z)$ where, for thermal fission of ^{235}U, κ is

$$\kappa = 2.43\left(\frac{\text{neut.}}{\text{fiss.}}\right)\left(3.1\times 10^{10}\right)\left(\frac{\text{fiss. s}^{-1}}{\text{Watt}}\right) = 7.53\times 10^{10}\left(\frac{\text{neut. s}^{-1}}{\text{Watt}}\right) \tag{1}$$

The fast fission neutrons quickly slow and diffuse away from their point of birth. Consider a thin disk source in fuel rod k of radius r, thickness dz about z, and strength 1 fn cm^{-3} that produces an energy-dependent fluence $\widehat{R}^k_i(z,E)$ at position $\mathbf{r}_i$ in the moderator. Here $\widehat{R}^k_i(z,E)$ is normalized to a unit fission-neutron emission density, i.e., to 1 fn cm^{-3} in the disk source. Then the total flux at position $\mathbf{r}_i$ produced by neutrons emitted by fuel rod k is expressed as[2]

$$\phi^k(\mathbf{r}_i,E) = \int_0^{z_{\max}} S^k_{\mathrm{fn}}(z)\widehat{R}^k_i(z,E)\pi r^2 \mathrm{d}z, \tag{2}$$

where $\widehat{R}^k_i(z,E)$ is the *fuel-rod fluence kernel* and has units of neutron cm^{-2} MeV^{-1} fn^{-1}. Because $S^k_{\mathrm{fn}}(z) = \kappa u^k(z)$, the total energy-dependent flux at detector location $\mathbf{r}_i$ from all K fuel rods is

$$\phi(\mathbf{r}_i,E) = \kappa\pi r^2 \sum_{k=1}^{K}\int_0^{z_{\max}} u^k(z)\widehat{R}^k_i(z,E)\mathrm{d}z. \tag{3}$$

The count rate C_i in the i-th MPFD is then given by

$$C_i = \int_0^{E_{\max}} \eta_i V_i \sum_f^i (E)\phi(\mathbf{r}_i,E)\mathrm{d}E = \int_0^{E_{\max}} m_i\eta_i\left(N_f/\rho\right)\sigma^i_f(E)\phi(\mathbf{r}_i,E)\mathrm{d}E, \tag{4}$$

where $E_{\max}$ is the maximum fission-neutron energy, η_i is the expected number of counts per fission event occurring in detector i, and V_i, m_i and (N_f/ρ) are the volume, mass and converter atoms per unit mass of the fissionable converter

[2] The time-delay between the fissions and the resulting flux at the detector locations is negligibly small ($\leq$milliseconds) and is ignored. In general, for normal reactor power transients, the slowing and diffusion times can be neglected.

material in detector i, respectively. Finally, $\sigma_f^i(E)$ and $\sum_f^i(E)$ are the microscopic and macroscopic cross-sections, respectively, of the converter material.

Combining Eqs. (3) and (4) gives the relationship between the unknown power-density profiles $u^k(z)$ and the detector count rates C_i, namely

$$C_i = Q_i \sum_{k=1}^{K} \int_0^{z_{\max}} R_i^k(z) u^k(z) \mathrm{d}z, \quad i = 1, \ldots, N_\mathrm{d}, \tag{5}$$

where $Q_i \equiv \kappa m_i \eta_i \pi r^2$ and the *MPFD response function* is

$$R_i^k(z) \equiv \left(N_f/\rho\right) \int_0^{E_{\max}} \sigma_f^i(E) \widehat{R}_i^k(z,E) \mathrm{d}E. \tag{6}$$

Eq. (5) is the key relation between the detector response and the power-density profiles. The quantity $Q_i R_i^k(z)$ can be interpreted as the count rate recorded in detector i, per unit power density at elevation z of fuel-rod k per unit differential elevation dz. This response function contains the entire physics of neutron transport, core geometry and composition, and detector characteristics. Its evaluation requires detailed transport calculations and is the subject of the present study.

2.2. Formulation of the inversion problem

The solution of the Fredholm integral equations of Eq. (5) for the K unknown power-density profiles $u^k(z)$ is a classic inversion problem. The reader is referred to Press et al. (1992) for general inversion techniques and to Shultis (2005) for details of the linear regularization scheme used in the present study. Here only a brief summary of the inversion technique used is presented.

To estimate the power-density profiles, Eq. (5) is first approximated by a set of linear algebraic equations for the power densities $u_j^k \equiv u^k(z_j)$, at M equidistant elevations $z_j = (j-1)\Delta z, j = 1, \ldots, M$ where $\Delta z = z_{\max}/(M-1)$, using an appropriate numerical quadrature scheme. The resulting equations have the form

$$C_i = \sum_{k=1}^{K} \sum_{j=1}^{M} R_{ij}^k u_j^k, \quad i = 1, \ldots, N_\mathrm{d}, \tag{7}$$

where the R_{ij}^k are the elements of an $N_\mathrm{d} \times M$ matrix. Because there are M unknown power-density values for each fuel rod, the total number of unknowns for K fuel rods is KM. The N_d equations of Eq. (7) can then be written compactly in matrix form as

$$\mathbf{C} = \mathbf{R}\mathbf{u} \tag{8}$$

where the response function matrix $\mathbf{R}$ is $N_\mathrm{d} \times KM$ in dimension and $\mathbf{u}$ is a $KM \times 1$ vector.

The evaluation of the matrix-elements R_{ij}^k of Eq. (7) depends on the specific quadrature scheme used. For the present study, a *piece-wise quadratic approximation* was used to calculate these matrix-elements (Shultis, 2005).

2.2.1. The linear regularization method

The unknown power-density profiles can be estimated by solving the linear algebraic equations given by Eq. (8). One way to solve these equations is to minimize the difference between the expected and measured data as measured by the χ^2 statistic. If $\mathbf{u}$ is a possible solution for Eq. (8), then χ^2 can be written as

$$\chi^2 = \sum_{i=1}^{N_\mathrm{d}} \frac{1}{\sigma_i^2} \left[C_i - \sum_{j=1}^{KM} R_{ij} u_j \right]^2 = |\mathbf{A}\mathbf{u} - \mathbf{b}|^2. \tag{9}$$

Here the covariances, covar $[C_i, C_j]$, are zero because neutron interactions in different detectors are uncorrelated, and σ_i is the standard deviation of the i-th detector's count rate C_i. The matrix $\mathbf{A}$ has elements $A_{ij} = R_{ij}/\sigma_i$ and the vector $\mathbf{b}$ has elements $b_i = C_i/\sigma_i$.

The inversion of Eq. (8) when $N_d < KM$ is an underdetermined problem since the number N_d of detector responses is smaller than the KM unknown power densities (at M locations in each of the K fuel rods). Shultis (2005) used the linear regularization technique, whereby a quadratic smoothness constraint is imposed on the solution of Eq. (8), so that KM linear equations are obtained for the KM unknowns u_i^k.

Linear regularization involves a minimization of the sum of two positive functionals $\mathcal{A}[\mathbf{u}]$ and $\mathcal{B}[\mathbf{u}]$, where $\mathcal{A}[\mathbf{u}]$ is the measure of the agreement of the solution to the measured data, expressed by $\chi^2 = |\mathbf{Au} - \mathbf{b}|$. The second functional is $\mathcal{B}[\mathbf{u}] = \mathbf{u^T Hu}$, where $\mathbf{H}$ is a *smoothing matrix*, and is chosen as a measure of smoothness of each of the $u^k(z)$. For example, if one believes that a quadratic function is a good approximation for $u^k(z)$ then the third derivative should be very small. With the use of forward finite differences, the following non-negative quantity for fuel rod k should be minimized

$$\int_0^{z_{\max}} \left[u^{k'''}(z)\right]^2 \mathrm{d}z \propto \sum_{j=1}^{M-3} \left[-u_j^k + 3u_{j+1}^k - 3u_{j+2}^k + u_{j+3}^k\right]^2. \tag{10}$$

$\mathbf{B}^k$ is the $(M-3)\times M$ matrix

$$\mathbf{B}^k = \begin{pmatrix} -1 & 3 & -3 & 1 & 0 & 0 & 0 & \dots & 0 \\ 0 & -1 & 3 & -3 & 1 & 0 & 0 & \dots & 0 \\ \vdots & & & & \ddots & & & & \vdots \\ 0 & \dots & 0 & 0 & -1 & 3 & -3 & 1 & 0 \\ 0 & \dots & 0 & 0 & 0 & -1 & 3 & -3 & 1 \end{pmatrix}, \tag{11}$$

from which the $M \times M$ symmetric matrix $\mathbf{H}^k = (\mathbf{B}^k)^T \mathbf{B}^k$ is obtained. Finally, the smoothing matrix $\mathbf{H}$ is a block diagonal matrix whose diagonal blocks are the $\mathbf{B}^k, k = 1, \dots, K$. Similar smoothing matrices can be formed for any degree of polynomial smoothing (Press et al., 1992), but quadratic smoothing was found adequate for this study.

The minimization of $\mathcal{A}[\mathbf{u}] + \lambda\mathcal{B}[\mathbf{u}]$ can produce a unique and generally realistic solution for $\mathbf{u}$ (Press et al., 1992). As the value of the Lagrange multiplier λ varies from 0 to ∞, the solution of $\mathbf{u}$ varies along the trade-off curve between minimizing $\mathcal{A}$ and minimizing $\mathcal{B}$.

The normal equations, whose solution minimizes $\mathcal{A}[\mathbf{u}] + \lambda\mathcal{B}[\mathbf{u}]$, are (Press et al., 1992)

$$\left(\mathbf{A}^T\mathbf{A} + \lambda\mathbf{H}\right)\mathbf{u} = \mathbf{A}^T\mathbf{b}. \tag{12}$$

These KM linear algebraic equations in KM unknowns can readily be solved using standard techniques such as the lower–upper (LU) decomposition method (Press et al., 1992). As an initial value of λ Press et al. (1992) suggest

$$\lambda = \frac{\mathrm{Tr}\left(\mathbf{A}^T\mathbf{A}\right)}{\mathrm{Tr}(\mathbf{H})}, \tag{13}$$

where Tr is the trace of a matrix (sum of diagonal elements). The value of λ is then iteratively made as small as possible to give the best agreement between the solution and the data. However, if λ is made too small, the regularization effect of $\mathcal{B}[\mathbf{u}]$ is lost because of computer round off errors and numerical instability arises.

3. Modeling the KSU reactor core

The KSU TRIGA reactor is a water moderated and cooled thermal reactor operated at a maximum steady state thermal power of 250 kW. The core upper grid plate has 90 large penetrations, each 3.81 cm in diameter into which fuel rods, experiments or control rods may be inserted. This aluminum grid plate also has smaller flux probe holes each 0.813 cm in diameter which allow the MPFDs to be placed inside the core. The fuel rods have a 3.63-cm inner diameter and a 3.74-cm outer diameter. The cladding and end fixtures are of stainless steel. The fuel meat consists of 20% enriched uranium in a zirconium hydride matrix ($ZrH_{1.65}$) and has a length $z_{\max} = 38.1$ cm. Fuel composition is 8.5% uranium and 91.4% $ZrH_{1.65}$ and has a density of 5.996 g/cm^3. Between the fuel ends and the fuel-rod end fixtures are cylindrical plugs of graphite.

The TRIGA core configuration has a symmetry in fuel rod arrangements. This symmetric feature allows the core to be conceptually divided into 60° segments. To reduce the computational and experimental efforts, the wedge-shaped

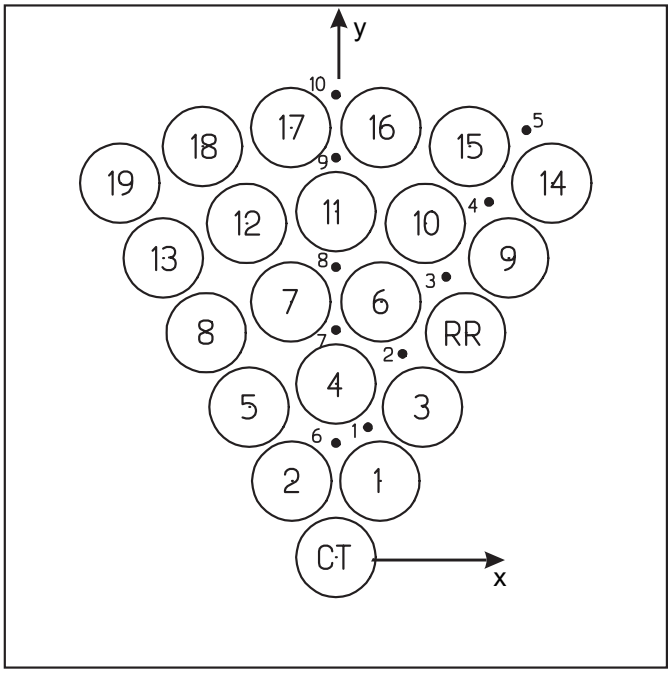

Fig. 1. Segment of the KSU TRIGA MARK II water-moderated reactor modeled in this study. The large circles with numbers are the fuel rods and the small solid circles are the probe holes. Also shown are the central thimble (CT) and the regulating control rod (RR).

segment of the core containing, 19 fuel rods and 10 probe holes and shown in Fig. 1, was selected for MPFD analysis and modeling in this study.

3.1. Calculation of the response function $R_i^k(z)$

Ideally suited to the task of calculating the detector response function $R_i^k(z)$, as given by Eq. (6), is the MCNP code (MCNP, 1997). This Monte Carlo code, besides being able to treat complex geometries, has the capability of estimating directly the right-hand side of Eq. (6).

3.1.1. Modifying the tally

In this study of the response of the MPFDs, the detectors themselves were not modeled. Rather, the point and ring detectors (F5 tallies of MCNP) were used to calculate the fluence at a detector location. Normally the energy-dependent fluence $\widehat{R}_i^k(z,E)$ at detector location $\mathbf{r}_i$ per source fission neutron emitted at elevation z in fuel rod k is tallied. However, use of the `FMn A M R1` card produces a tally of the form

$$\text{tally} = A\int_0^{E_{\max}} \sigma_{R1}^M(E)\widehat{R}_i^k(z,E)\mathrm{d}E. \tag{14}$$

This is precisely the form of Eq. (6) with the constant $\mathtt{A} = (N_f/\rho)$, the material number `M` is for the detector fissionable material, and the reaction number $\mathtt{R1} = -6$ for the total fission cross-section. Here the units of N_f are in $\mathrm{b}^{-1}\,\mathrm{cm}^{-1}$ so that the response function tally has units of fission per gram of fissionable material in the MPFD. For ^{232}Th and ^{235}U lined MPFDs the constant $\mathtt{A} = N_f/\rho$ has the value 0.002562 and 0.002596 $\mathrm{b}^{-1}\,\mathrm{g}^{-1}\,\mathrm{cm}^2$, respectively.

3.1.2. MCNP geometry models for the response function

For the KSU TRIGA it is planned to deploy a vertical string of five MPFDs in each probe hole of the core segment shown in Fig. 1. The MPFDs are to be equally spaced vertically with a detector opposite to each end of the fuel meat (see Fig. 2). Then, with a detailed geometric model of a single TRIGA fuel rod and by using the universe feature of MCNP, it is possible to replicate this single fuel rod in all the fuel rod holes in the study segment. In all cases room temperature was assumed and the fuel rods were surrounded by an effective water medium, i.e., the problem boundary was placed far from the regions of interest. No reflecting surfaces were employed since point and ring tallies were used.

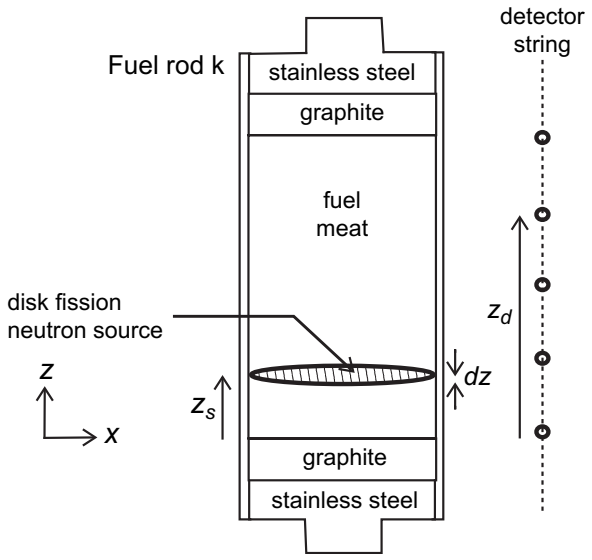

Fig. 2. Schematic diagram of the one fuel rod model to determine the detector response function $R_i^k(z)$. The fuel rod is surrounded by an infinite water medium at room temperature. Not to scale.

However, such a ''brute force'' calculation is computationally very expensive since the needed variance reduction techniques would have to be tailored to every MPFD location and to every fission source elevation in every fuel rod. Rather, an approach was adopted in this study that allowed the use of simplified geometric models with only fuel rods very near the detector considered. In the hydrogen TRIGA moderator (both the water and the $ZrH_{1.65}$) fission neutrons thermalize within several centimeters from their point of birth and diffuse only a few more centimeters before they are absorbed. Thus, fuel rods distant from an MPFD can be expected to have negligible on the detector's response. Similarly, fission neutrons born at an elevation z_s much greater than the MPFD elevation z_d can also be expected to be of minor importance compared to those neutrons born near the detector elevation.

In the sections below, example calculations are presented to verify these expectations and to show that a simplified model using only the fuel rods near an MPFD can be used to estimate the response function $R_i^k(z)$ with reasonable computational expense.

Finally, it should be mentioned that in all the MCNP results shown below the `NONU` command was used to prevent the creation of secondary fission neutrons during the simulations, as is required from the definition of the detector response function.

3.1.2.1. A single fuel rod model. To investigate how the relative heights of the source and detector affect the response function, a single fuel rod, as shown in Fig. 2, was used. Muliple MCNP runs were made, each with the disk source at a different elevation z_s in the fuel rod and with an array of ring detectors at various elevations z_d. In this manner, the response function $R_i^k(z_s) \equiv R_i^k(z_d, z_s)$ was calculated. Here k refers to this single fuel rod and the detector position index i is for the MPFD at elevation z_d. The results are shown in Fig. 3 where $R_i^k(z_s)$ is shown as a function of the distance between the source and MPFD elevations, i.e., $|z_s - z_d|$. Observe that the response function varies by about six orders of magnitude over the 38.1 cm range of $|z_s - z_d|$ and that the largest MPFD response is for source neutrons born near the same elevation as the MPFD.

Except for sources near either end of the fuel meat, the response function is seen to be a smooth function of $|z_s - z_d|$. That sources near the ends of the fuel meat produce slightly different responses is not surprising since the replacement of fuel on one side by graphite, stainless steel and water can be expected to alter the nearby thermalization and diffusion of neutrons compared to neutrons born away from the ends.

3.1.2.2. An infinite fuel rod model. In another MCNP model, the fuel rod was allowed to extend to the problem boundary, tens of meters away from the regions containing the disk source and detectors. The response function for an infinitely long fuel rod is rigorously a function of only $|z_d - z_s|$ for any z_d and z_s. Hence, an infinite fuel-rod model can be used to calculate $R_{i\infty}^k(|z_{di} - z_s|)$ much more efficiently. This response function is a good approximation

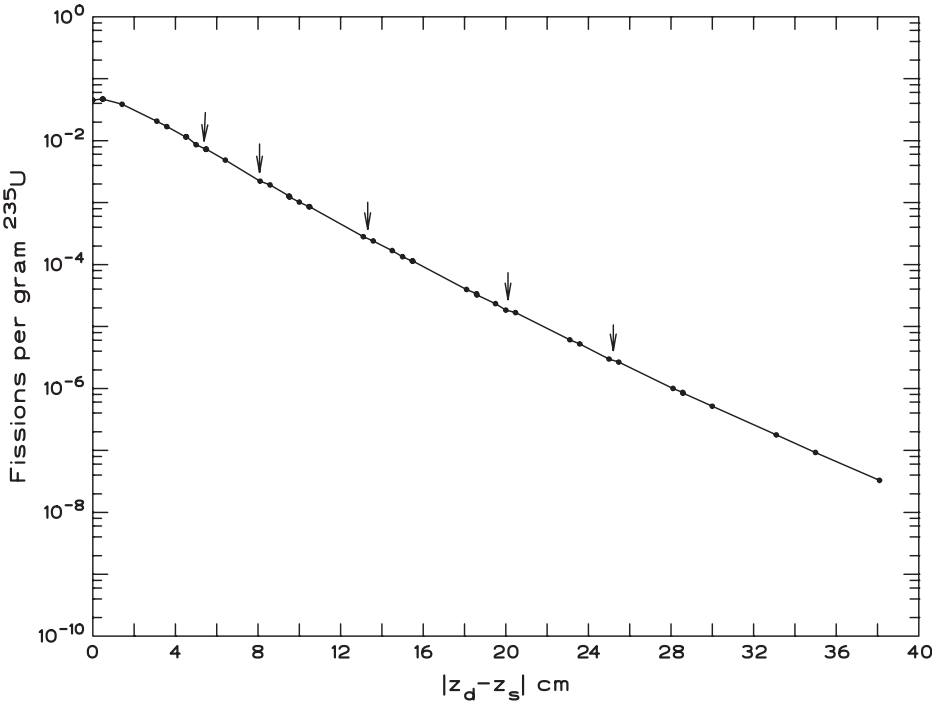

Fig. 3. The detector response function for a single finite fuel rod. The down arrows indicate that there are some irregular responses that deviate from the general smooth trend. These irregular points arise when z_s is near one of the ends of the fuel meat.

for the response function of an actual fuel rod except when z_s and/or z_d are near the ends of the fuel meat. Results for this infinite fuel-rod model are shown in Fig. 4 which exhibit none of the ''kinks'' that are in Fig. 3 for the finite fuel-rod model and that arise from sources near the ends of the fuel meat in the finite fuel-rod model.

3.1.2.3. The end correction factor. The infinite fuel-rod model is much simpler to use, and, thus, it was proposed to use this simpler model for response function calculations and to develop an *end correction factor* to correct the infinite fuel-rod model for the response function depression near the ends of the fuel meat.

First the response depressions at two ends of the fuel meat were studied for symmetry. To do so, the source and detector elevations were kept the same, i.e., $|z_d - z_s| = 0$ and z_d were then moved in small increments away from either end. Fig. 5 superimposes the results for z_d near the top and for z_d near the bottom. From this figure, it is seen that the responses near the top or bottom of a finite fuel rod are identical so that the same end correction factor can be used at both ends. Moreover, when more than about 5 cm away from either end, the end effect is negligible and the response for the infinite fuel-rod model can be used.

The five MPFDs in each probe hole are equally spaced and have elevations of 0.00, 9.53, 19.05, 28.58 and 38.1 cm. Because the end effect occurs only within about 5 cm of the ends of the fuel meat, only the two detectors adjacent to the ends are influenced by the end effect. For source elevations near the two ends, the infinite-rod response function $R^k_{i\infty}(|z_d - z_s|)$ can be corrected to give the proper finite-rod response $R^k_i(z_d, z_s) \equiv R^k_i(z_s)$ by multiplying the infinite-rod response function by an end correction factor, i.e.,

$$R^k_i(z_d, z_s) = \epsilon(\Delta z) R^k_{i\infty}(|z_d - z_s|), \quad \begin{cases} \Delta z = z_s, & \text{if } z_d = 0 \\ \Delta z = z_{\max} - z_s, & \text{if } z_d = z_{\max} \end{cases} \tag{15}$$

The end correction factor for the top and bottom detectors in a string is thus calculated as

$$\epsilon(\Delta z) \equiv \frac{R^k_i(z_d, z_s)}{R^k_{i\infty}(|z_d - z_s|)}. \tag{16}$$

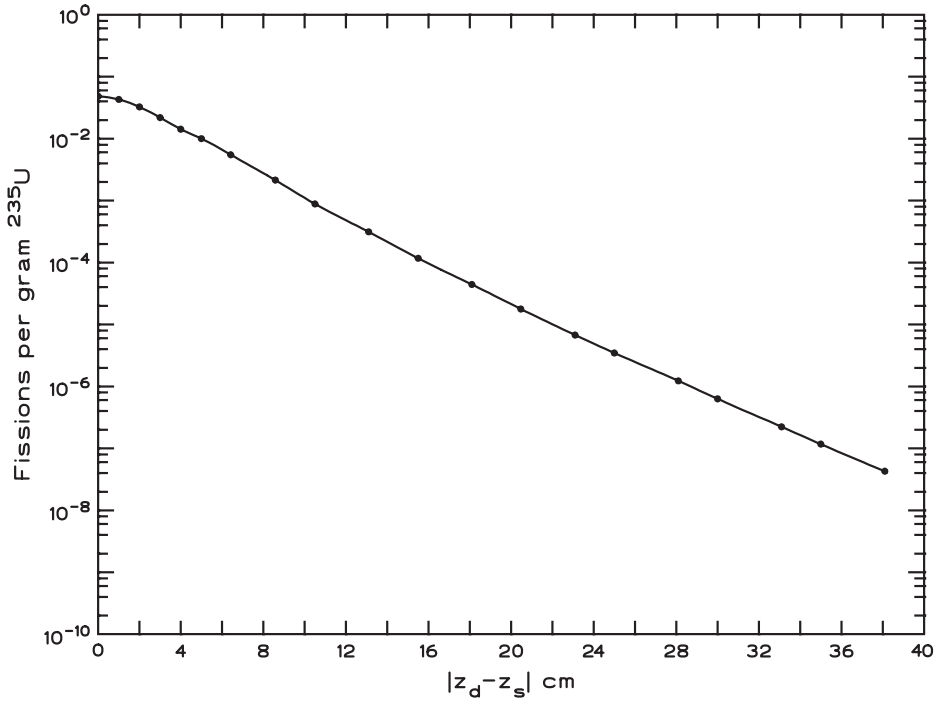

Fig. 4. The detector response function for a single infinite fuel rod.

To compute $\epsilon(\Delta z)$, the finite and infinite fuel-rod models were used to calculate $R_i^k(z_d = 0, z_s)$ and $R_{i\infty}^k(z_d = 0, z_s)$, respectively, over a fine grid of z_s values. The resulting end correction factor is shown in Fig. 6. The smooth line in this figure is the fitting approximation

$$y = a + bx^2 + cx^4 + dx^6 + ex^8, \tag{17}$$

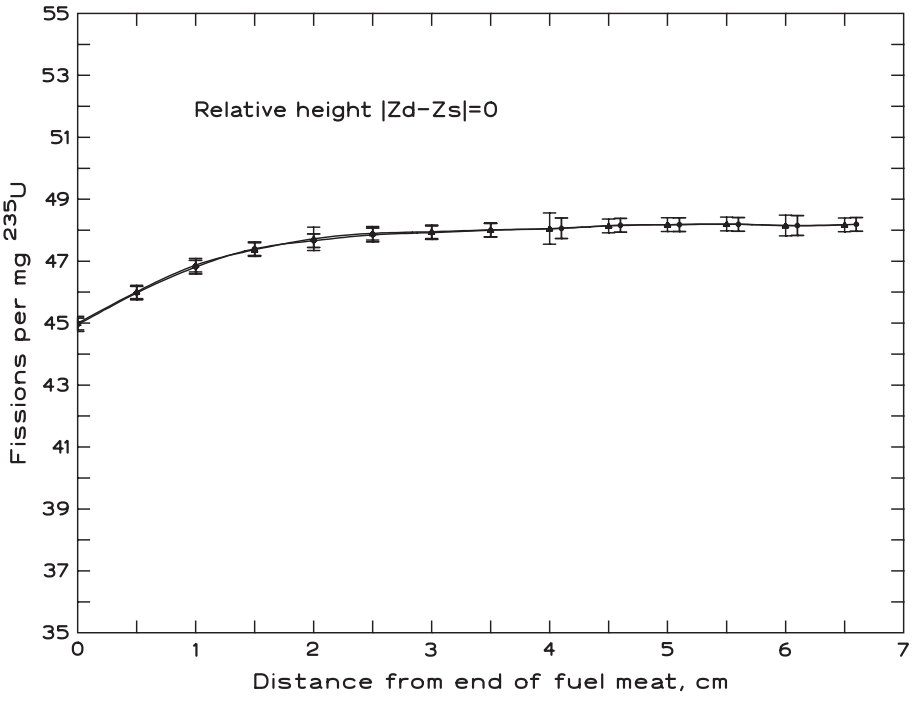

Fig. 5. Comparison of the response depressions at the top and bottom ends of a single finite fuel rod showing the symmetry of the depression.

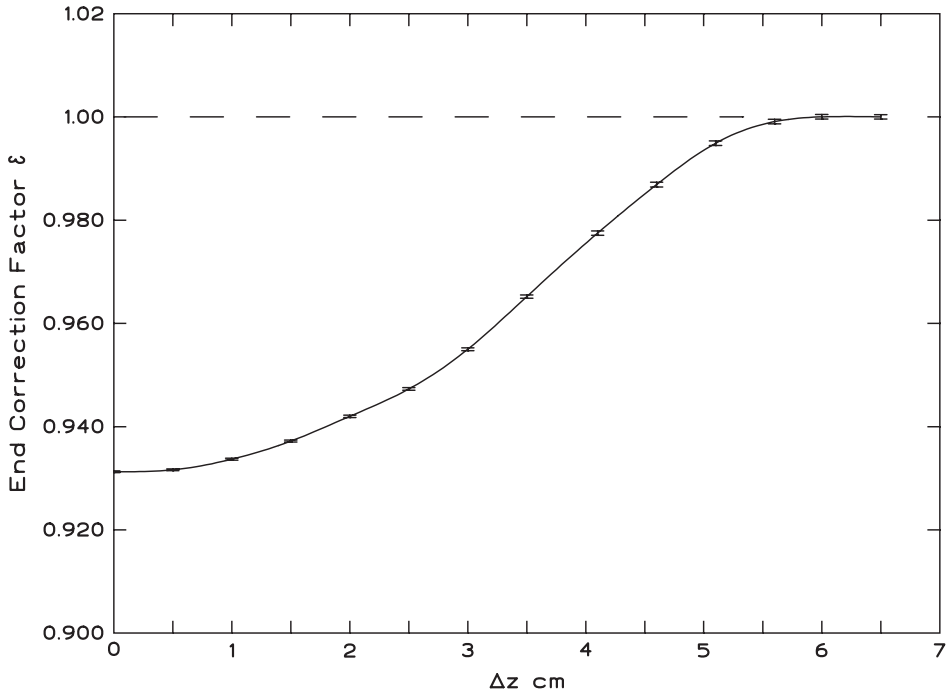

Fig. 6. The end correction factor calculated from Eq. (16) for a finite and an infinite fuel rod at the end region.

where the coefficients are $a = 0.931357780$, $b = 0.00225379230$, $c = 7.850058100 \times 10^{-5}$, $d = 3.5039901 \times 10^{-6}$, and $e = 2.975174 \times 10^{-08}$. This empirical result can then be used for detectors at both ends of the fuel meat because of the symmetry in the end effect.

3.1.2.4. Cluster rod model. Because fission neutrons slow and diffuse over relatively small distances from their point of birth, neutrons have little chance of reaching a detector located far from their birth sites. To determine which fuel rods are important to the response of a particular probe-hole detector string, a cluster fuel-rod model was developed. In this model infinite fuel rods were successively added to the MCNP calculation starting with the nearest fuel rod, then to the next nearest, and so on. As more fuel rods are included in the simulation the response function increases. Eventually, however, the addition of a distant fuel rod produces a negligible increase in the response. An example of the cluster model results is shown in Fig. 7.

With this cluster fuel-rod model, the number and IDs of the fuel rods that had the most influence on detectors in each probe hole were determined by multiple MCNP calculations in which successively more neighboring fuel rods were added to the cluster model until additional fuel rods had negligible influence on the detectors' responses. Hence, Eq. (5) is simplified to

$$C_i = Q_i \sum_{k=1}^{K_i} \int_0^{z_{\max}} R_i^k(z) u^k(z) \mathrm{d}z, \quad i = 1, \ldots, N_\mathrm{d}, \tag{18}$$

where the summation is now over the K_i fuel rods that contribute significantly to the count rate C_i of the i-th detector. The IDs and number of the fuel rods that contribute almost all the response to an MPFD in a given probe hole are listed in Table 1.

A comparison for probe hole 1 is shown in Fig. 8 for the four nearest fuel rods using the finite and infinite fuel-rod models. The resulting MPFD response functions are slightly higher with a maximum difference of about 22% at $|z_d - z_s| = z_{\max}$. When the end correction factor is applied to the infinite fuel-rod results, the two results become almost identical.

3.1.3. Empirical equations for MPFD detector response functions

The Table Curve Program (Jandel, 1991) was used to fit empirical equations to the response function data obtained from the MCNP calculations. Table Curve fits thousands of possible equations, but those equations that fit the data

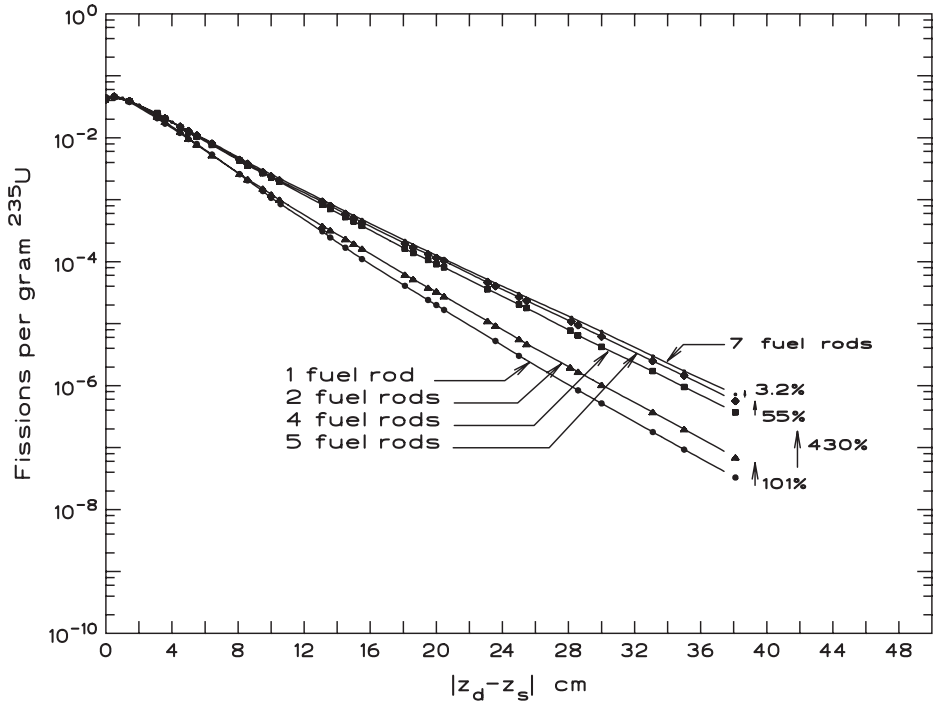

Fig. 7. The effect of successively adding neighboring infinite fuel rods for detectors in probe hole 1. The disk source was in fuel rod 1. The sixth and seventh nearest fuel rods have little additional effect compared to that produced by the five nearest fuel rods. Similar results were obtained for all probe holes.

well were simple in form, and had the fewest number of fitting parameters (generally less than six) were selected. Thus, for each fuel rod in the contributing cluster for each probe hole (see Table 1) an empirical detector response function was obtained. These empirical equations then permit rapid calculation of $R_i^k(z)$ for any detector. A listing of the empirically fit equations and associated FORTRAN subroutines is given by Ahmed (2006).

4. Estimating power-density profiles

The eventual intent of the present initiative was to use MPFD experimental data to estimate the power-density profiles in the fuel rods of the KSU TRIGA reactor. However, experimental data are not yet available. Consequently, to determine the capabilities of the proposed linear regularization inversion method using the detector response functions developed in this study, simulated MPFD count rate data were generated for both thermal-neutron and fast-neutron MPFDs.

To generate simulated data, the idealized and fictitious power-density profiles $u^k(z)$, proposed earlier by Shultis (2005), were used. The simulated count rate C_i was evaluated from Eq. (5) using adaptive Gaussian numerical quadrature and also from Eq. (7). Both approaches gave the same simulated count rate data within five significant figures, an indication that the discretization approximation used to develop Eq. (7) introduces little approximation error. It is interesting to note that the C_i for the ^{235}U MPFDs were thousands of times greater than for ^{232}Th MPFDs.

Table 1
The number and ID of the principal fuel rods affecting an individual probe hole

Probe hole ID	Fuel rod ID	Probe hole ID	Fuel rod ID
1	1,2,3,4,5	6	1,2,3,4,
2	3,4,6,7	7	4,6,7,11
3	6,9,10,11	8	6,7,10,11,12
4	9,10,14,15	9	10,11,12,16,17
5	9,10,14,15	10	11,16,17

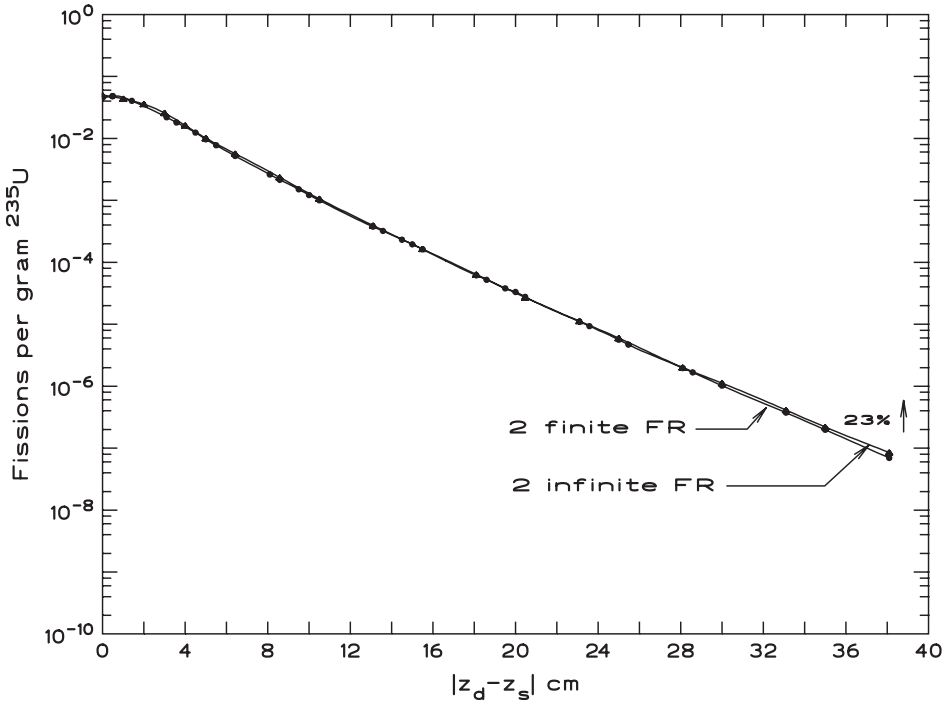

Fig. 8. Comparison of detector response functions for probe hole 1 obtained with four finite and infinite fuel rods. The source was in fuel rod 1.

The power-density profiles $u^k(z)$ were calculated at $M = 11$ equispaced elevations in each fuel rod. An example is shown in Fig. 9 of the estimated power-density profiles for 10 fuel rods at $KM = 110$ locations using simulated data from an array of 50 ^{235}U MPFDs (five MPFDs in each of 10 probe holes). The idealized profiles used to generate the simulated data are shown by the solid lines and the estimated values by the small solid circles. The method appears to be quite robust giving nearly identical excellent results for λ ranging from 10^2 to 10^{-7}. However, if λ is made too small

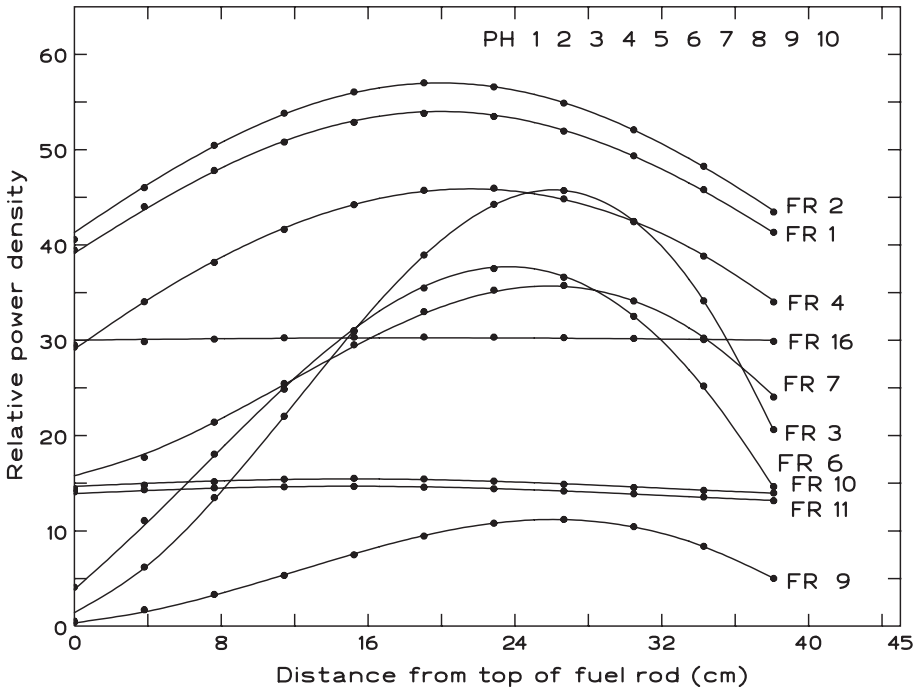

Fig. 9. Idealized power-density profiles (solid line) and unfolded results (solid circles) for 10 fuel rods (FRs) and 10 probe holes (PHs) with five ^{235}U MPFDs in each probe hole. The term "relative power density" refers to the fact that the test profiles had arbitrary units.

the regularization produced by the smoothness constraint is lost to round off error and numerical instabilities arise. Likewise if λ is made very large, the quadratic smoothness constraint forces the estimated profiles to become more parabolic in shape. Finally, the fast-neutron ^{232}Th MPFD data, although quite different in magnitude, produce indistinguishable from those of Fig. 9.

In practice, the fast-neutron MPFDs may be of greatest interest for power mapping since the fast-flux distribution is determined by fission sources much nearer the detector than is the thermal flux. Also control motion has less of an effect on the fast flux than it does on the thermal flux.

It is not surprising that good agreement is obtained for self-consistent simulation and reconstruction. Of future interest is the effect of noise in the data and systematic errors that can arise in experimental data such as detector positioning errors, different responses among the detectors, etc. In the experimental phase of this project, such questions are to be investigated.

5. Conclusions

Initial tests with MPFDs demonstrate their capability of performing near-core and in-core operations quite effectively (McGregor et al., 2005). Presently, efforts are underway to deploy an array of MPFDs in the KSU TRIGA core to allow real-time 3D flux and power mapping. Key to the unfolding of the resulting MPFD data is an accurate set of response functions for these detectors. Using the Monte Carlo MCNP code it has been demonstrated that such response functions can be obtained by using simpler infinite fuel-rod models with an appropriate end correction to give the response functions for finite fuel rods.

Because the MPFD's response must necessarily exhibit statistical fluctuations and electronic noise, and it is very important to take these non-ideal responses into account when assessing the robustness of the present methodology. Thus, future study needs to address the robustness of the inversion technique for data exhibiting varying amounts of uncertainty and noise. Also the effect of control motion near probe hole detectors needs to be investigated.

From the results presented in this paper, it is apparent that linear regularization method is quite successful at inverting simulated in-core MPFD responses to calculate power-density profiles for the reactor core. Further, the MCNP code with appropriate simplified models can effectively generate the key response functions needed for 3D power and flux mapping of a reactor core.

Acknowledgements

This work was supported under the Department of Energy Research Initiative (NERI) Grant DE-FG07-02SF22611.

References

Ahmed, A.S.M.S., 2006. Determining Axial Fuel-rod Power Density Profiles from In-core Neutron Flux Measurements, MS thesis, Department of Mechanical and Nuclear Engineering, Kansas State University, Manhattan, Kansas.

Jandel Scientific, 1991. Table Curve. Version 3.0. Jandel Scientific, Corte Madera, CA.

McGregor, D.S., Ohmes, M.F., Ortiz, R.E., Ahmed, A.S.M.S., Shultis, J.K., 2005. Micro-pocket fission detectors (MPFD) for in-core neutron flux monitoring. Nucl. Instr. Meth. A 554, 494.

MCNP: A general Monte Carlo N-particle Transport Code, 1997. Version 4C, LA-12625-M, Los Alamos.

Press, W.H., Teukolsky, S.A., Vetterling, W.T., Flannery, B.P., 1992. In: Numerical Recipes, second ed. Cambridge University Press, New York.

Shultis, J.K., 2005. Determining axial fuel-rod power density profiles from in-core neutron flux measurements. Nucl. Instr. Meth. A 547, 663.